



Surface-specific interaction by structure-match confined pure high-energy facet of unstable $\text{TiO}_2(\text{B})$ polymorph

Guolei Xiang, Yang-Gang Wang, Jun Li, Jing Zhuang & Xun Wang

Department of Chemistry, Tsinghua University, Beijing 100084, China.

SUBJECT AREAS:

COLLOIDS

SURFACES, INTERFACES AND THIN FILMS

TWO-DIMENSIONAL MATERIALS

CHEMICAL PHYSICS

Received
4 December 2012

Accepted
22 February 2013

Published
11 March 2013

Correspondence and requests for materials should be addressed to

J.L. (junli@tsinghua.edu.cn) or X.W. (wangxun@mail.tsinghua.edu.cn)

Surface structures and surface interactions are key factors that influence the reactivity and stability of nanomaterials. Combining experimental and theoretical investigations, we illustrate the roles of surface interactions in the formation and phase stability of an unusual $\text{TiO}_2(\text{B})$ polymorph that preferentially exposes the plane of the highest surface energy. We find that the favorable bidentate adsorption of ethylene glycol on the $\text{TiO}_2(\text{B})(010)$ plane enables the formation and confines the phase stability of $\text{TiO}_2(\text{B})$ ultrathin nanosheets. The essence of such selective generation of the unusual nanostructure with ultrahigh purity both in phase and morphology lies in the specific adsorption driven by the matched interface structures. The general roles of structural match for the activity and stability in physical interactions are elucidated.

Control over phase and morphology of nanomaterials is a key method in improving their performance¹. During the preparation and processing of nanocrystals, both growth and phase stability are inherently dominated by thermodynamics, especially on a nanometer scale^{2,3}. With decreasing particle size, surface energy becomes the most important parameter that dictates the phase stability of nanocrystals^{3,4}. It has been revealed that the phase stability and transformation of common TiO_2 polymorphs (rutile, anatase and brookite) are size-dependent; the most stable phase above 35 nm is rutile, but the reversed surface energy makes anatase the most stable phase below 11 nm³. It is well recognized that stable equilibrium shapes of nanocrystals are determined by intrinsic lattice symmetries and the relative order of surface energies of all crystalline facets^{5,6}. Though surface energy largely controls the growth process of crystals, it is still possible to realize shape-controlled synthesis of many nanocrystals in solution by introducing various additives, e.g., ions, surfactants and polymers, to change the growth rates along different orientations^{1,7–11}. In these processes, certain growth planes are favored due to the selective adsorption of additive molecules¹¹. This provides kinetic approaches to control the growth of nanocrystals by introducing selective or non-selective interactions on the surfaces. Many materials can now be synthesized with well-controlled sizes and shapes^{1,8,10,11}.

As an important semiconducting oxide, TiO_2 has been widely studied in the fields of heterogeneous catalysis¹², photocatalysis^{13,14}, photovoltaics¹⁵, etc., involving three major phases¹⁶. We previously developed a facile method to prepare ultrathin nanosheets of $\text{TiO}_2(\text{B})$, an unusual phase of TiO_2 , via a one-step solvothermal reaction¹⁷. Through the procedure, 1-nm thick sheets with a high exposure percentage of (010) planes can be readily obtained. However, the nature of the surface interactions in the formation of this metastable phase and in preferential exposure of the (010) plane have been elusive. Herein we investigate the surface interactions of $\text{TiO}_2(\text{B})$ with different solvents to reveal the underlying mechanism of its formation and phase stability. Through a combined experimental and theoretical study, we have found that the stability of this unusual phase with 2D shape is confined by the structure-matched specific interactions on a special crystalline facet. Structural match at different scales is an important mechanism to control specific interactions or processes with definite results, e.g., molecule recognition¹⁸, and sometimes they are also described in terms of specificity or selectivity. Here we emphasize that it is the structure-matched specific interaction between ethylene glycol (EG) molecules and $\text{TiO}_2(\text{B})$ over the (010) plane that drives the formation and stability of the special phase with an ultrathin 2D morphology.



Results

Synthesis of TiO₂(B) Nanosheets. TiO₂(B) was prepared by directly hydrolyzing TiCl₃ or TiCl₄ in ethylene glycol at 150°C. All the products are uniform 2D nanosheets as shown in Figures 1a–b. The phase character was compared with TiO₂(B) nanowires prepared by hydrothermal method and characterized by means of powder X-ray diffraction (XRD) and Raman spectroscopy, which confirm the pure phase of TiO₂(B) (Figures 1c–d and S1). Index of the exposed facet was analyzed from a high resolution TEM image (HRTEM) and the corresponding Fourier transformation pattern (Figure 1e). The spots were assigned to 200 and 001, and the angle between them was measured to be 73°, identical to the angle between the reciprocal space axes of *a** and *c** (Figure S2). We further quantified the amount of EG in the product using differential thermal analysis (DTA) and thermogravimetric analysis (TGA) ranging from 25°C to 800°C in air (Figure 1f). EG were completely eliminated at 465°C with a residual weight of 73%. From the TGA and DTA results the total amount of EG on the surface of TiO₂(B) nanosheets is estimated to be around 22% by weight (see Figure S3 for more details).

The above results show that TiO₂(B) nanosheets can be effectively prepared in EG with high selectivity of phase and morphology. Through contrast experiments we found that TiO₂(B) phase could only be directly prepared in EG, while only anatase or the mixture of anatase and rutile were obtained in other hydroxylic solvents, e.g. H₂O, CH₃OH, C₂H₅OH. Thus EG is an indispensable component for the formation of TiO₂(B). We infer that a strong interaction must exist between EG molecules and TiO₂(B)(010) plane that dominates the formation of this unusual phase.

Elucidating the Growth Mechanism by Computational Modeling.

To gain insight into the underlying formation mechanism of the TiO₂(B) nanosheets, we studied the interactions of EG molecules with TiO₂ polymorphs through periodic density functional theory (DFT) calculations using the Quickstep code of CP2K package^{19,20}. We systematically studied possible interaction patterns between EG and TiO₂(B) by exploring all possible adsorption configurations on the (010) plane. As EG is a bis-hydroxyl compound, both the monodentate and bidentate adsorption configurations on

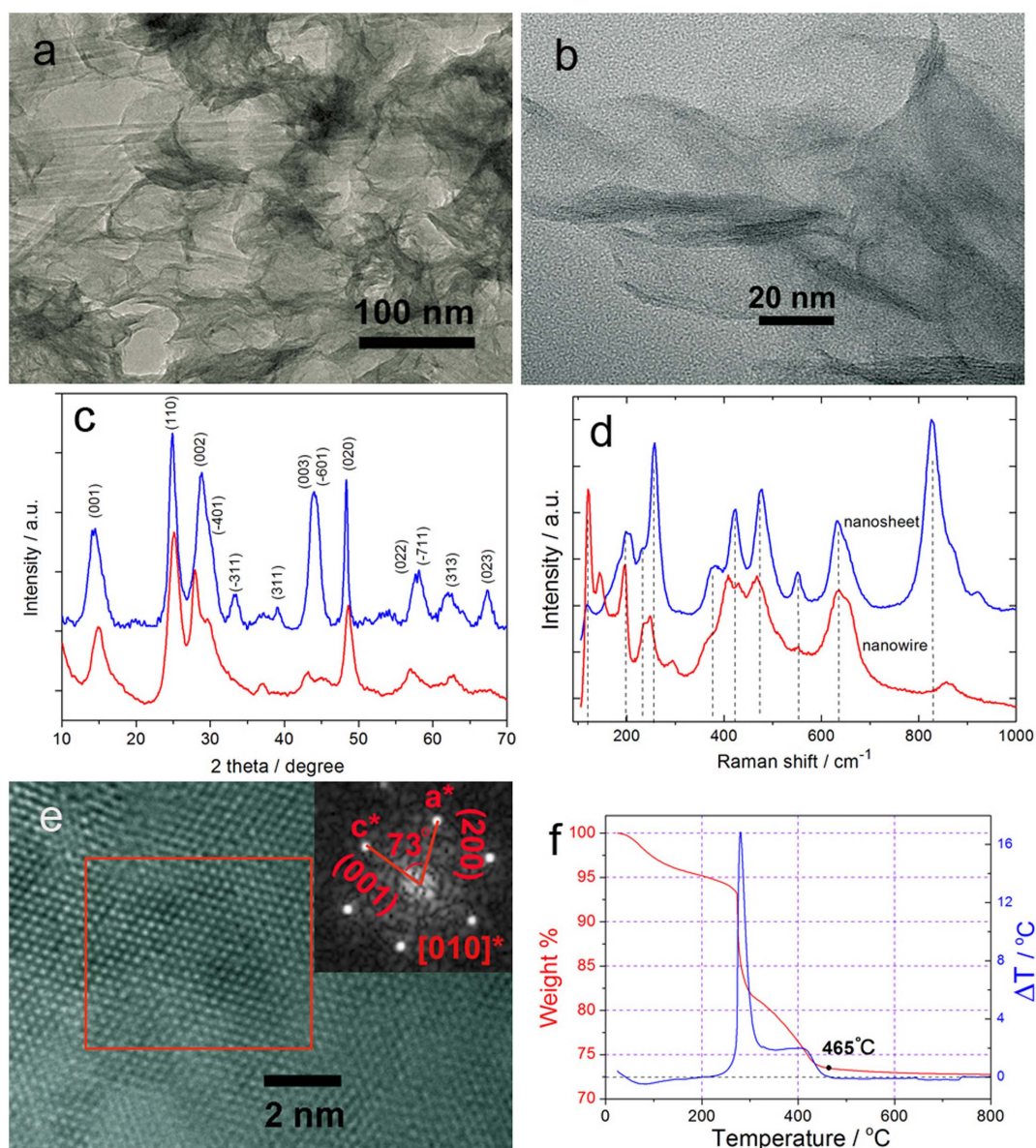


Figure 1 | (a–b) TEM images of TiO₂(B) nanosheets. (c–d) XRD and Raman spectra confirming the phase purity of TiO₂(B) nanosheets in comparison with that of nanowires. (e) HRTEM and Fourier transformation images for determining the surface index. (f) TGA and DTA data characterizing the amount of EG in TiO₂(B) nanosheets.



TiO₂(B)(010) facet were investigated (see Figure 2 for the configuration models).

The geometry optimizations show that for the monodentate adsorption the EG molecule remains in the “chair” configuration as in the gas phase, while for bidentate adsorption the configuration of the EG molecule transforms from “chair” to “boat” configuration to bind with two Ti sites. The calculated adsorption energies for the *dissociative* configurations (Figure 2c–d) are significantly more negative than those for *molecular* configurations (Figure 2a–b), indicating that the EG molecules are more favorable to adsorb onto TiO₂(B) (010) facet through dissociative configurations. The dissociative adsorption energies are -1.92 eV (or -0.96 eV per Ti site) for the bidentate configuration and -0.95 eV for the monodentate configuration. These results indicate that the configuration change does not decrease the binding strength of each OH group with the surface Ti sites. It is therefore feasible for EG to interact with the TiO₂(B)(010) plane using both hydroxyl groups to form the most stable configuration. This strong bidentate interaction accounts for the fact that TiO₂(B) can only be synthesized in EG with exposure of a specific (010) plane.

To corroborate this conclusion, we further considered the interactions of EG with TiO₂(B) (001) and (110) planes, which are intrinsically more stable than TiO₂(B) (010) plane in vacuum and in a humid environment^{21–23}. In view of the high reaction temperature, EG molecules are assumed to dissociate after adsorption on these TiO₂(B) facets and the saturated adsorptions are considered in EG solvent. The calculated average adsorption energies per EG molecule on (010), (001), (110) planes (Table 1) are -1.41 , 0.19 , -1.22 eV, respectively, confirming the EG molecule binds more favorably to (010) plane compared to the others providing a thermodynamic template to form the (010) plane. We also investigated the surface stability in terms of the change of surface energies (γ) before and after EG adsorption. For the bare planes without EG adsorption, (001) is the most stable plane with the lowest surface energy, and the order of the surface stability follows (001) > (110) > (010), consistent with previous calculations²¹. The least stable plane (010), however, can be greatly stabilized in EG solvents and becomes more stable than (001) and (110) planes, which agrees well with our experimental results that (010) is the solely exposed plane. We further considered the interactions of EG with other polymorphs of TiO₂, anatase and rutile, although neither are formed during the synthesis of TiO₂ in EG. As the common planes for the two phases are (101), (100), (001) for anatase and (110), (100), (111) for rutile, they were chosen to compare with TiO₂(B) (010) plane. All the adsorption energies for the saturated bidentate adsorptions of EG on the planes of anatase and

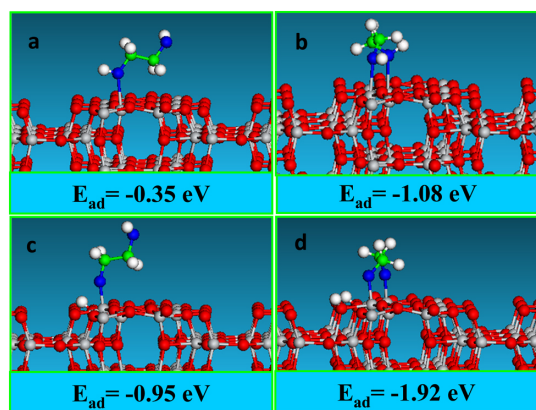


Figure 2 | Adsorption configurations and energies of EG on TiO₂(B) (010) plane from DFT calculations: (a) molecular monodentate adsorption (b) molecular bidentate adsorption (c) dissociative monodentate adsorption and (d) dissociative bidentate adsorption.

Table 1 | Adsorption energies (AEs) for EG saturated adsorption on different planes of TiO₂(B), anatase, and rutile, and the surface energies for TiO₂(B)

TiO ₂ (B)	AEs (eV)	γ without EG (Jm ⁻²)	γ with EG (Jm ⁻²)
010	-1.41	0.93	0.33
001	0.19	0.62	0.76
110	-1.22	0.83	0.35
Anatase	AEs (eV)	Rutile	AEs (eV)
101	-1.19	110	-0.93
100	0.20	101	-1.12
001	-0.78	111	-1.08

rutile are found to be less stable than on TiO₂(B)(010) plane (Table 1). This result suggests that the bidentate binding structures of the EG molecules on either anatase or rutile surfaces are less stable than that with TiO₂(B) (010), consistent with the rare phase preference for the later. Clearly the strong bidentate interaction makes EG a specific solvent to generate TiO₂(B) polymorph exposing a plane with the highest surface energy. The structure-match interaction likely dominates the selective formation of ultrathin TiO₂(B) nanosheets with highly pure phase.

Solvent effects on phase stability of TiO₂(B) nanosheets. Compared with anatase and rutile, TiO₂(B) is a less stable phase of TiO₂. To determine the stability of this metastable polymorph in the forms of ultrathin nanosheets, we investigated its phase transformation behaviors in the solid state and in different solvents. The results were monitored via XRD and Raman spectroscopy (Figure 3). Through the temperature-dependent tests by heat-treating the samples for 5 h in solid state, the nanosheets preserved the metastable phase up to 250°C, but it gradually transformed into anatase phase above 300°C. Pure anatase was obtained at 500°C, and only a little amount of rutile appears at 800°C (Figure 3a). To prepare TiO₂(B) nanowires, hydrogen titanate needs to be treated at 400°C, and they start to transform into anatase at 600°C (Figure S4). Thus TiO₂(B) nanosheets are less stable than nanowires, because the phase transition temperature is reduced by almost 300°C.

On the other hand, the phase stability of the TiO₂ nanosheets depends on the chemical environment of the solvent (Figure 3b–c). The TiO₂ material was prepared in EG by adding H₂O to hydrolyze Ti precursor. The products formed by hydrolysis were separated by centrifugation and washed with the respective solvents, EG and ethanol (EtOH), to minimize the influence of any residual water on the results. Control experiments showed the nanosheets after postprocess in either EG or EtOH preserve the initial phase at temperatures up to 200°C, but are transformed into anatase when 0.5 mL water was introduced into ethanol. The results show that the metastable structure is quite sensitive to water. Through systematic tests we checked the phase stability in pure water and found anatase phase appeared above 55°C. Typical results showing good degrees of crystallization after heating at 60 and 70°C for 15 h are shown in the XRD and Raman spectra (Figures 3b–c). There is also a diffraction peak of the intermediate transitional phase in the XRD pattern.

The key factor dominating different roles of the three solvents in the phase transformation results of TiO₂(B) nanosheets appears to be their different interaction strengths with TiO₂(B) (010) plane, that is H₂O > EG > EtOH. To confirm this, the interactions of ethanol, EG, and water molecules with TiO₂(B) (010) surfaces were investigated computationally. Inasmuch as the phase transformation experiments were conducted in bulk solvents, the coverage density of these solvent molecules on the surface is very high, as revealed from the TGA results (Figure 1d). Therefore, the saturation adsorption configurations with all Ti sites occupied by the solvent molecules are used to model the experimental conditions (Figure 4). The calculated

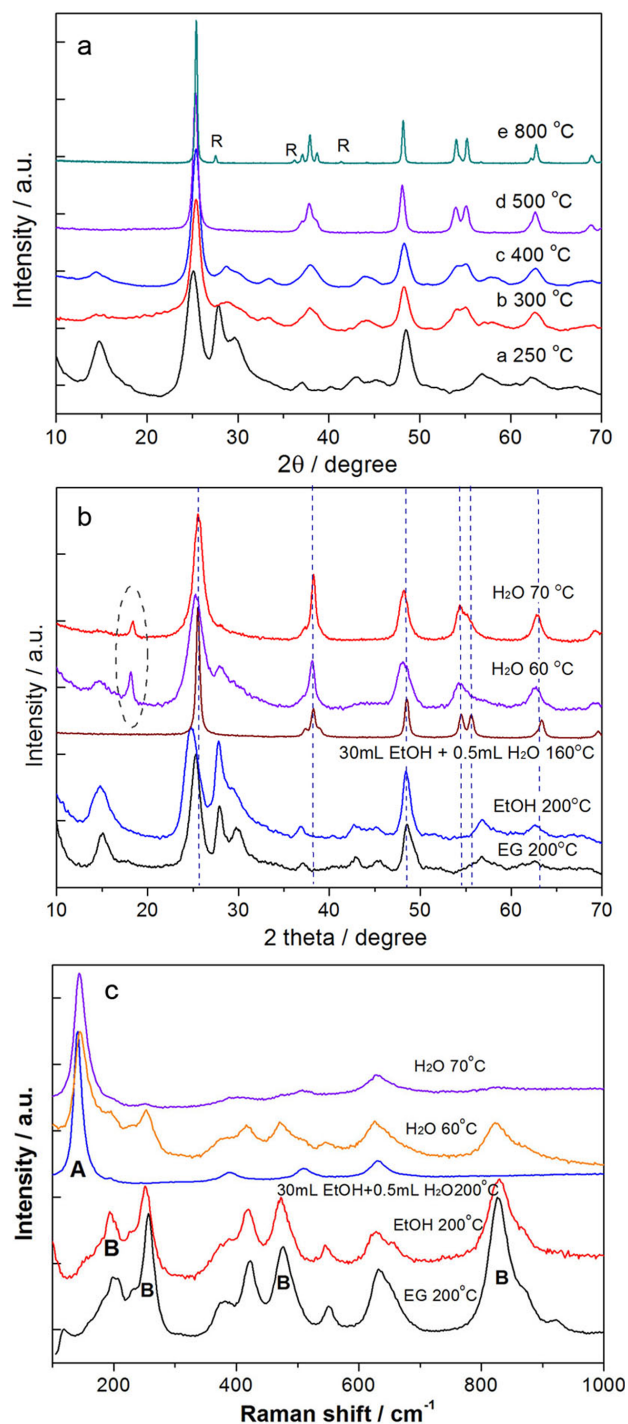


Figure 3 | Phase stability of $\text{TiO}_2(\text{B})$ nanosheets in solid state and in solvents. (a) Phase evolution at different temperatures in solid states. (b–c) Phase stability in different solvents, ethylene glycol (EG), ethanol (EtOH) and water (H_2O) monitored via XRD and Raman spectra.

average adsorption energies of each Ti site for ethanol, EG, and water molecules (-0.56 eV, -0.70 eV and -0.81 eV, respectively, Figure 4d) indicate that it is thermodynamically plausible for water to replace EG molecules, but it is difficult for ethanol molecules to replace EG. The difference in the binding strength of different solvents can be partly attributed to the steric hindrance effects, which deter efficient adsorption of solvent molecules onto the surface of $\text{TiO}_2(\text{B})$ nanosheets. As a highly polar molecule, water has the strongest adsorption energy due to its smaller size and the lower

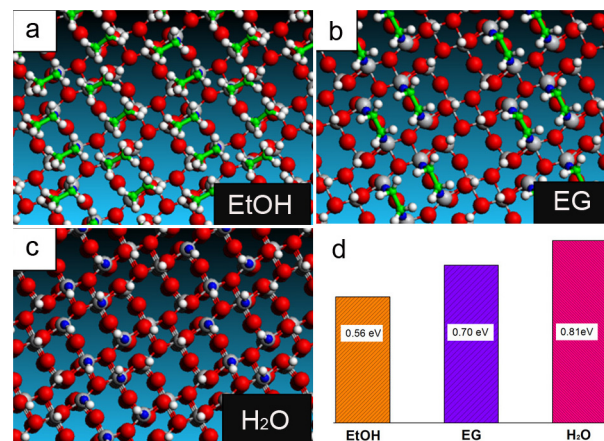


Figure 4 | Models of $\text{TiO}_2(\text{B})(010)$ planes with saturated adsorption by solvent molecules used in the DFT calculations. (a) ethanol adsorption. (b) bidentate ethylene glycol adsorption. (c) water adsorption. (d) average energies per Ti sites for ethanol, EG, and water molecules from DFT calculations.

steric interaction to the adjacent counterparts. The EG molecules can occupy two Ti sites by bidentate adsorption to decrease the steric hindrance, thus having lower adsorption energy than the ethanol molecules.

Discussion

For the formation, phase stability and evolution of inorganic nanocrystals, many examples have been reported from the aspects of surface structure and particle size^{24–30}. Using the models of TiO_2 and ZnS, the importance of surface interactions with solvents, ions and impurities is emphasized for the phase stability and transformation processes. The essence lies in altering the energy states of nanocrystals by modifying the surface structures through certain interactions that can affect the thermal stability of nanocrystals under specific circumstances. Since it is a surface-initiating process, phase transformation can be adjusted by changing the surface states. Similarly, it is possible to realize phase transition of nanocrystals by modifying their surfaces via the adsorption or desorption of solvent molecules or impurity ions.

In the current work, we illustrate the roles of surface-specific interaction in the formation and phase stability of an unusual $\text{TiO}_2(\text{B})$ nanosheet. The bidentate adsorption of EG on the (010) plane is shown to enable the formation and confine the phase stability of $\text{TiO}_2(\text{B})$. Such a relatively stable state of this metastable polymorph is generated by the matched size and configuration on the surface. Thus through the surface-specific interaction, the $\text{TiO}_2(\text{B})$ (010) plane can be effectively stabilized under the particular chemical environment. Based on the phase transformation and DFT results, we conclude that EG is a phase-stabilizer for $\text{TiO}_2(\text{B})$ nanosheets due to bidentate adsorption configurations over the (010) facet. The high ratio of surface adsorbed EG, up to 22% by weight, also indicates a strong binding interaction. On the contrary, water is a potent destabilizer of the $\text{TiO}_2(\text{B})$ phase and favors the formation of anatase. As ethanol binds more weakly than EG on the surface of $\text{TiO}_2(\text{B})$, it fails to change the energy state of $\text{TiO}_2(\text{B})$ or to induce phase evolution.

In general, the specific interaction with structural match as illustrated herein is an important mechanism to analyze the processes with high specificity and selectivity. The underlying driving force is the matched factors at a particular scale. In the physical interactions involving the existence and state evolution of matter, the configuration match of size and shape is an important and potentially dominating factor that induces specific pathways with high

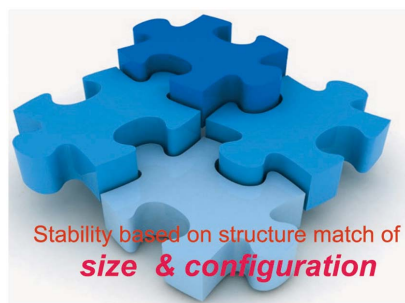


Figure 5 | Schematic illustration of the roles of structure-match based on size and configuration on the stability and activity in physical interactions. (The authors hold the copyright for fig. 5 and would like to release it under an open access license).

selectivity. Due to the confinement effects of specific interactions, some unstable active states can be preserved as illustrated in Figure 5.

In summary, we have elucidated the formation and stability mechanisms of the unusual TiO₂(B) polymorph by combined experimental and theoretical investigations. The ultrathin nanosheets exposing (010) planes, confined by the bidentate interaction of EG with Ti sites, result from the surface-specific interaction with a structural match. Our work provides an example showing how specific interactions on a structure-matched surface can influence the selective generation of nanocrystals with high purity both in phase and morphology. The roles of structural match on activity and stability in physical interactions are particularly highlighted.

Methods

Synthesis of TiO₂(B) nanosheets. In a typical synthetic procedure, 1 mL TiCl₃ aqueous solution or 1 mL TiCl₄ and 1 mL deionized water were mixed with 30 mL ethylene glycol in a 40 mL Teflon-lined autoclave. After stirring for 30 s with a glass rod, the mixture was sealed and heated in an oven to 150 °C for 6 h. The products were separated by centrifugation and washed four times with water and ethanol.

Synthesis of TiO₂(B) nanowires. 3.0 g P25 TiO₂ was added to a 10 M aqueous solution of NaOH. After stirring for 1 h the resulting suspension was transferred to a teflon-lined autoclave and heated to 180 °C for 15 h. The product was acid-washed by stirring the sample in 0.1 M HCl solution for 24 h. The material was then filtered, washed with distilled water, and dried at 80 °C for 15 h. TiO₂(B) nanowires were prepared by heating the acid-washed titanate nanowires at 400 °C for 4 h in air.

Phase transformation of TiO₂(B) nanosheets in solvents. To investigate the effect of different solvents, i.e., EG, water, and ethanol, on the phase transformation of the nanosheets prepared in EG we isolated the products by centrifugation and then washed the products with related solvents 5 times. The experiments were conducted in teflon-lined autoclaves in an oven for EG and ethanol and in glass flasks heated in a water bath for water.

Characterization. Crystal structures of the as-prepared samples were determined from X-ray diffraction (XRD) patterns, were recorded on a Rigaku diffractometer using Cu K α radiation ($\lambda = 1.5418 \text{ \AA}$), operating at 40 kV and 200 mA and a scanning rate of 6° per minute. Morphologies of the products were investigated on a high-resolution transmission electron microscopy (HRTEM) of FEI Tecnai F20 with an accelerating voltage of 200 kV.

Computational details. All calculations were performed using supercell DFT methods as implemented in the Quickstep code of the CP2K package^{19,20}. Spin-polarized Kohn-Sham formalism was adopted. The exchange-correlation energy used the generalized-gradient approximation (GGA) with Perdew-Burke-Ernzerh (PBE) functional³¹. With the mixed basis sets, the localized double- ζ Gaussian basis sets were used to describe the valence orbitals of the atoms in the cell and the plane waves were expanded with a cutoff energy of 350 Rydberg³². Core electrons have been modeled by scalar relativistic norm-conserving pseudopotentials with 12, 6, 4 and 1 valence electrons for Ti, O, C, and H, respectively^{33,34}. The Brillouin zone integration were performed with a reciprocal space mesh consisting of only the Gamma point. In the geometry optimizations, the total energies and the maximum forces were converged to 0.001 eV and 0.01 eV/Å, respectively. The calculated lattice parameters, $a = b = 3.82 \text{ \AA}$, $c = 9.59 \text{ \AA}$ for anatase, $a = b = 4.65 \text{ \AA}$, $c = 2.99 \text{ \AA}$ for rutile, and $a = 12.32 \text{ \AA}$, $b = 3.79 \text{ \AA}$, $c = 6.60 \text{ \AA}$, $\beta = 106.95^\circ$ for TiO₂-B, are within 2% offset from the experimental results^{35,36}, indicating that the theoretical approach is appropriate. In our calculations, large supercells were used to model the planes of TiO₂(B) and of rutile and anatase crystals. All the slabs were repeated periodically with a vacuum spacing of 15 Å between the surfaces of the supercells.

The adsorption energy of EG is calculated according to: $E_{ads} = (E_{slab+EG} - E_{slab} - E_{EG})$, where E_{slab} denotes the energy per surface unit cell of the specified slab model with n bulk unit cells, $E_{slab+EG}$ the total energy of the adsorption complex including the relaxed surface and the adsorbate EG molecule, and E_{EG} the energy of the isolated EG molecule. The surface energy without EG adsorption is calculated using $\gamma = (E_{slab} - nE_{bulk})/2A$, where E_{bulk} is the energy per unit cell of TiO₂(B), A the area of the surface, and n the number of the TiO₂ unit cell contained in the slab surface. The surface energy with saturated adsorption of EG is calculated as $\gamma = (E_{slab+mEG} - nE_{bulk} - mE_{EG})/2A$, where m is the number of EG molecules binding to the slab surface and $E_{slab+mEG}$ is the total energy of slab surface with EG molecules saturatedly adsorbing on the two sides of the slab.

- Burda, C., Chen, X. B., Narayanan, R. & El-Sayed, M. A. Chemistry and properties of nanocrystals of different shapes. *Chem. Rev.* **105**, 1025–1102 (2005).
- Navrotsky, A., Mazeina, L. & Majzlan, J. Size-driven structural and thermodynamic complexity in iron oxides. *Science* **319**, 1635–1638 (2008).
- Zhang, H. Z. & Banfield, J. F. Understanding polymorphic phase transformation behavior during growth of nanocrystalline aggregates: Insights from TiO₂. *J. Phys. Chem. B* **104**, 3481–3487 (2000).
- El-Sayed, M. A. Small is different: Shape-, size-, and composition-dependent properties of some colloidal semiconductor nanocrystals. *Acc. Chem. Res.* **37**, 326–333 (2004).
- Xiang, G. L., Shi, X. J., Wu, Y. L., Zhuang, J. & Wang, X. Size effects in atomic-level epitaxial redistribution process of RuO₂ over TiO₂. *Sci. Rep.* **2**, 801 (2012).
- Wang, Z. L. Transmission electron microscopy of shape-controlled nanocrystals and their assemblies. *J. Phys. Chem. B* **104**, 1153–1175 (2000).
- Wang, X., Zhuang, J., Peng, Q. & Li, Y. D. A general strategy for nanocrystal synthesis. *Nature* **437**, 121–124 (2005).
- Zhuang, Z. B., Peng, Q. & Li, Y. D. Controlled synthesis of semiconductor nanostructures in the liquid phase. *Chem. Soc. Rev.* **40**, 5492–5513 (2011).
- Zhou, Z. Y., Tian, N., Li, J. T., Broadwell, I. & Sun, S. G. Nanomaterials of high surface energy with exceptional properties in catalysis and energy storage. *Chem. Soc. Rev.* **40**, 4167–4185 (2011).
- Tao, A. R., Habas, S. & Yang, P. D. Shape control of colloidal metal nanocrystals. *Small* **4**, 310–325 (2008).
- Yang, H. G. *et al.* Anatase TiO₂ single crystals with a large percentage of reactive facets. *Nature* **453**, 638–641 (2008).
- Valden, M., Lai, X. & Goodman, D. W. Onset of catalytic activity of gold clusters on titania with the appearance of nonmetallic properties. *Science* **281**, 1647–1650 (1998).
- Li, B. *et al.* Ultrafast interfacial proton-coupled electron transfer. *Science* **311**, 1436–1440 (2006).
- Onda, K. *et al.* Wet electrons at the H₂O/TiO₂(110) surface. *Science* **308**, 1154–1158 (2005).
- Gratzel, M. Photoelectrochemical cells. *Nature* **414**, 338–344 (2001).
- Chen, X. & Mao, S. S. Titanium dioxide nanomaterials: Synthesis, properties, modifications, and applications. *Chem. Rev.* **107**, 2891–2959 (2007).
- Xiang, G. L., Li, T. Y., Zhuang, J. & Wang, X. Large-scale synthesis of metastable TiO₂(B) nanosheets with atomic thickness and their photocatalytic properties. *Chem. Commun.* **46**, 6801–6803 (2010).
- Klarner, F. G. & Kahlert, B. Molecular tweezers and clips as synthetic receptors. Molecular recognition and dynamics in receptor-substrate complexes. *Acc. Chem. Res.* **36**, 919–932 (2003).
- CP2K. <http://cp2k.berlios.de>, 2010.
- VandeVondele, J. *et al.* QUICKSTEP: Fast and accurate density functional calculations using a mixed Gaussian and plane waves approach. *Comput. Phys. Commun.* **167**, 103–128 (2005).
- Vittadini, A., Casarin, M. & Selloni, A. Structure and stability of TiO₂-B surfaces: A density functional study. *J. Phys. Chem. C* **113**, 18973–18977 (2009).
- Vittadini, A. *et al.* Stability of TiO₂ polymorphs: exploring the extreme frontier of the nanoscale. *Chem. Phys. Chem.* **11**, 1550–1557 (2010).
- Vittadini, A., Casarin, M. & Selloni, A. Hydroxylation of TiO₂-B: insights from density functional calculations. *J. Mater. Chem.* **20**, 5871–5877 (2010).
- Zhang, H. Z., Gilbert, B., Huang, F. & Banfield, J. F. Water-driven structure transformation in nanoparticles at room temperature. *Nature* **424**, 1025–1029 (2003).
- Chernyshova, I. V., Hochella, M. F. & Madden, A. S. Size-dependent structural transformations of hematite nanoparticles. 1. Phase transition. *Phys. Chem. Chem. Phys.* **9**, 1736–1750 (2007).
- Huang, F. & Banfield, J. F. Size-dependent phase transformation kinetics in nanocrystalline ZnS. *J. Am. Chem. Soc.* **127**, 4523–4529 (2005).
- Levchenko, A. A., Li, G. S., Boerio-Goates, J., Woodfield, B. F. & Navrotsky, A. TiO₂ stability landscape: Polymorphism, surface energy, and bound water energetics. *Chem. Mater.* **18**, 6324–6332 (2006).
- Chen, B., Zhang, H. Z., Gilbert, B. & Banfield, J. F. Mechanism of inhibition of nanoparticle growth and phase transformation by surface impurities. *Phys. Rev. Lett.* **98**, 106103 (2007).
- Lin, Z., Gilbert, B., Liu, Q. L., Ren, G. Q. & Huang, F. A thermodynamically stable nanophase material. *J. Am. Chem. Soc.* **128**, 6126–6131 (2006).



30. Finnegan, M. P., Zhang, H. Z. & Banfield, J. F. Phase stability and transformation in titania nanoparticles in aqueous solutions dominated by surface energy. *J. Phys. Chem. C* **111**, 1962–1968 (2007).
31. Perdew, J. P., Burke, K. & Ernzerhof, M. Generalized gradient approximation made simple. *Phys. Rev. Lett.* **77**, 3865–3868 (1996).
32. Lippert, B. G., Hutter, J. & Parrinello, M. A hybrid Gaussian and plane wave density functional scheme. *Mol. Phys.* **92**, 477–488 (1997).
33. Goedecker, S., Teter, M. & Hutter, J. Separable dual-space Gaussian pseudopotentials. *Phys. Rev. B* **54**, 1703–1710 (1996).
34. Krack, M. Pseudopotentials for H to Kr optimized for gradient-corrected exchange-correlation functionals. *Theor. Chem. Acc.* **114**, 145–152 (2005).
35. Yahia, M. B. *et al.* Updated references for the structural, electronic, and vibrational properties of TiO₂ (B) bulk using first-principles density functional theory calculations. *J. Chem. Phys.* **130**, 204501 (2009).
36. Diebold, U. The surface science of titanium dioxide. *Surface science reports* **48**, 53–229 (2003).

Acknowledgements

This work was supported by NSFC (91127040, 20921001) and the State Key Project of Fundamental Research for Nanoscience and Nanotechnology (2011CB932402).

Author contributions

G.L.X. and Y.G.W. contributed equally to this work. G.L.X. conducted the experimental parts and Y.G.W. performed the DFT calculations. J.Z. contributed to the characterization processes. J. L. was responsible for the theoretical work. X.W. conceived and designed the work and was responsible for the work. All authors discussed the results, wrote and commented on the manuscript.

Additional information

Supplementary information accompanies this paper at <http://www.nature.com/scientificreports>

Competing financial interests: The authors declare no competing financial interests.

License: This work is licensed under a Creative Commons Attribution-NonCommercial-NoDerivs 3.0 Unported License. To view a copy of this license, visit <http://creativecommons.org/licenses/by-nc-nd/3.0/>

How to cite this article: Xiang, G.L., Wang, Y.-G., Li, J., Zhuang, J. & Wang, X. Surface-specific interaction by structure-match confined pure high-energy facet of unstable TiO₂(B) polymorph. *Sci. Rep.* **3**, 1411; DOI:10.1038/srep01411 (2013).